Journal of Materials Chemistry C

Accepted Manuscript

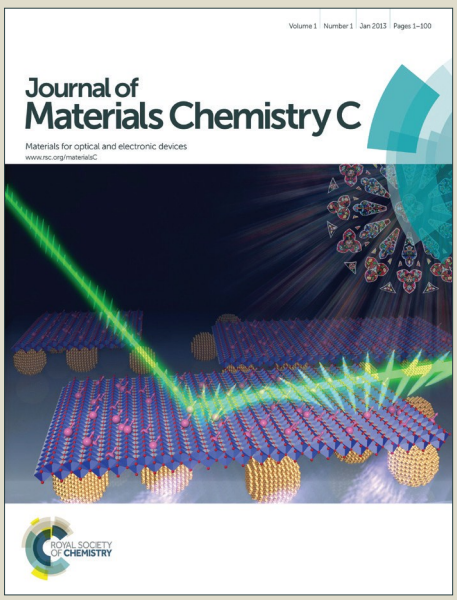

ROYAL SOCIETY OF CHEMISTRY

www.rsc.org/materialsC

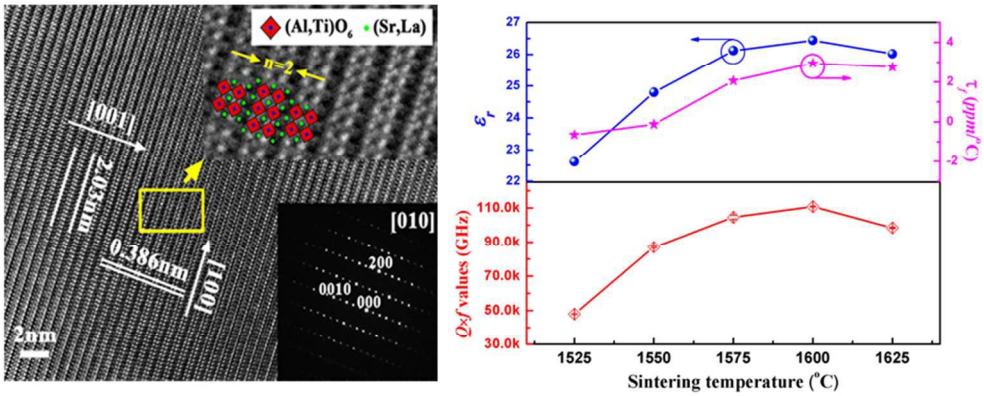

80x35mm (300 x 300 DPI)

Journal Name

ARTICLE

$Sr_2LaAlTiO_7$: A New Ruddlesden-Popper Compound with Excellent Microwave Dielectric Properties

Received 00th January 20xx,
Accepted 00th January 20xx

DOI: 10.1039/x0xx00000x

www.rsc.org/

Bing Liu[a], Xiao Qiang Liu[a] and Xiang Ming Chen[a]*

A new n = 2 type Ruddlesden-Popper compound $Sr_2LaAlTiO_7$ was synthesized and characterized, and the microwave dielectric properties were investigated together with their microstructures. X-ray diffraction (XRD) Rietveld analysis and selected area electron diffraction (SAED) patterns confirmed that these compounds belong to the *I*4/*mmm* space group with tetragonal crystal symmetry. The lattice parameters were calculated as $a = b = 3.840$ Å and $c = 20.270$ Å. The interlayer polarization was much lower than that of the previously reported $SrLa_2Al_2O_7$ ceramics, and a well ordered distribution of ions along *c* axis was confirmed from the high resolution transmission electron microscopy (HRTEM) images. The excellent microwave dielectric properties were obtained and the optimal combination ($\varepsilon_r = 26.5$, $Q\times f = 110{,}850$ GHz, $\tau_f = 2.95$ ppm/°C) was obtained for the sample sintered at 1600°C in air for 3h. Considering the merits of a simple preparation, less process sensitivity and most importantly, the comparatively cheap raw materials, $Sr_2LaAlTiO_7$ ceramics could be expected as a promising new candidate for ultra-low loss microwave dielectric ceramics.

1 Introduction

In the last decades, dielectric ceramics with proper dielectric constant ε_r, high quality factor Q (the inverse of dielectric loss) and near-zero temperature coefficient of resonant frequency (τ_f) have received wide academic and commercial attention because of the important applications for resonators, filter and other key components in microwave communication systems.[1,2] With the rapid development of microwave communication towards high-band microwave and millimeter wave range, ultra-low loss microwave ceramics are strongly required.[3–5] So far, $Ba(Mg_{1/3}Ta_{2/3})O_3$ ($\varepsilon_r = 25$, $Q\times f = 176{,}000$ GHz, $\tau_f = 2.7$ ppm/°C) has been recognized as the most important ultra-low loss microwave dielectric ceramic.[6] However, the poor sinterability, strong processing dependence of properties and high cost due to the expensive raw materials (Ta_2O_5) have cast doubts on their continued use in common microwave applications.[1,7–9] On the other hand, $MgTiO_3$–$CaTiO_3$ ceramics ($\varepsilon_r = 21$, $Q\times f = 56{,}000$ GHz, $\tau_f = 0$ ppm/°C) have the relatively low cost,[10] but their $Q\times f$ values are not high enough for high-band microwave and millimeter wave applications. Therefore, it is a challenge issue to search ultra-low loss microwave dielectric ceramic new systems with high performance combined with acceptable cost.

Recently, Ruddlesden-Popper (RP) compounds have attracted continuous scientific interests and represent an active area of research owing to their fascinating physical-chemistry properties.[11-14] The general formula of these compounds can be written as $(A,A')_{n+1}B_nO_{3n+1}$, and their structure can be considered to consist of n blocks of corner-sharing (BO_6) octahedral intergrown in an ordered way with a rock salt layer ((A,A')O) along *c* axis. In our previous work, $MLnAlO_4$ and $SrLn_2Al_2O_7$ (M = Sr, Ca, Ln = La, Nd, and Sm) ceramics with n = 1 & 2 RP structure have been proposed and their excellent microwave dielectric properties ($\varepsilon_r = 16 \sim 19$, $Q\times f = 54{,}600 \sim 69{,}500$ GHz, $\tau_f = -32 \sim -1$ ppm/°C for n = 1; $\varepsilon_r = 18.2 \sim 21.6$, $Q\times f = 64{,}680 \sim 71{,}680$ GHz and $\tau_f = -22.1 \sim +4$ ppm/°C for n = 2) were also obtained.[11–15] Besides, by systematically analyzing the structure, Fan and Yi et al. have found that the interlayer polarization of RP structure takes the major responsibility for the dielectric loss and

Laboratory of Dielectric Materials, School of Materials Science and Engineering, Zhejiang University, Hangzhou 310027, CHINA. E-mail: xmchen59@zju.edu.cn

Journal of Materials Chemistry C

further improvement of microwave dielectric properties could be expected by structural modifications.[11,13] Actually, this idea has been realized in M^{2+}/Ti^{4+} co-substituted $MLnAlO_4$ solid solution systems, where overall improvements of microwave dielectric properties (ε_r = 18.5 ~ 21.5, $Q\times f$ = 75,000 ~ 96,500 GHz, τ_f ~ 0 ppm/^{o}C) were achieved.[16–18] However, the microwave dielectric characteristics especially the $Q\times f$ value are still not good enough. Considering that the n = 2 $SrLn_2Al_2O_7$ ceramics generally exhibit higher ε_r and $Q\times f$ values when compared to $MLnAlO_4$ ceramics, more effective modification of the microwave dielectric characteristics should be expected. On the other hand, $SrLa_2Al_2O_7$ ceramics exhibit the best combination of microwave dielectric properties (ε_r = 18.2, $Q\times f$ = 71,680 GHz, τ_f = –22.1 ppm/^{o}C) among $SrLn_2Al_2O_7$ series, and their theoretical $Q\times f$ value (130,300 GHz) is about two times of the measured one.[11,19] Therefore, a significant improvement of microwave dielectric properties is expected in Sr^{2+}/Ti^{4+} co-substituted $SrLa_2Al_2O_7$ ceramics. However, only few members of the solid-solution system are thermodynamically stable and the synthesis of such layered oxides has become a major challenge. As a series of $Sr_2La(B_1^{3+}B_2^{4+})O_7$ (B_1 = Fe, Cr, B_2 = Mn, Ti) have been already investigated in the literature,[20–23] a new RP compound, $Sr_2LaAlTiO_7$, might be designed and prepared as a new candidate for ultra-low loss microwave dielectric ceramics.

In the work, $Sr_2LaAlTiO_7$ ceramics were prepared by a standard solid–state reaction method for the first time, and their microwave dielectric properties are evaluated together with the microstructures. Moreover, infrared reflectivity spectra analysis is conducted to understand their intrinsic dielectric properties.

2 Experimental methods

The synthesis of $Sr_2LaAlTiO_7$ complex oxide proceeded through the solid solution of two intermediate compounds $SrLa_2Al_2O_7$ and $Sr_3Ti_2O_7$ via a standard solid-state reaction method. The initial intermediate components were synthesized using high purity $SrCO_3$ (99.95%), La_2O_3 (99.99%), Al_2O_3 (99.99%) and TiO_2 (99.99%) oxide powders as raw materials. As rare earth oxide (La_2O_3) was hygroscopic, it was additionally preheated at 1000^{o}C for 2h before weighting. The corresponding stoichiometric raw powders of $SrLa_2Al_2O_7$ and $Sr_3Ti_2O_7$ were mixed and ball milled with zirconia media in alcohol for 24h and then calcined at 1600^{o}C and 1250 ^{o}C in air for 4h, respectively. After that, the two calcined components were mixed in a 1:1 molar ratio according to the nominal composition $Sr_2LaAlTiO_7$ and re-milled. The dried powders were then mixed with 4 wt% solution of polyvinyl alcohol (PVA) and pressed into disks of 12 mm in diameter and 2 – 6 mm in height. These disks were sintered at 1525 – 1625^{o}C in air for 3h to yield the dense ceramics. After sintering, the disks were cooled to 1100^{o}C at a rate of 2^{o}C/min, and further cooled inside the furnace.

The crystalline phase constitutions were identified by powder X-ray diffraction (XRD) (RIGAKU D/max 2550/PC, Rigaku Co., Tokyo, Japan) analysis with Cu$K\alpha$ radiation. The bulk density of the ceramics was measured by the Archimedes method. Microstructure of the polished and thermally etched surfaces of the sintered disks was characterized using scanning electron microscopy (SEM) (SIRION-100, FEI Co., Eindhoven, Netherlands). Thermal etching was conducted at a temperature 50^{o}C lower than the sintering temperature for 30 min. The XRD data for Rietveld analysis were collected over the range of 2θ = 8^o – 130^o with a step of 0.02^o and a count time of 2 s. The Rietveld structure calculation was carried out with the FULLPROF program.[24] Samples for transmission electron microscopy (TEM) observation were prepared by disaggregating the ceramics followed by grinding in an agate mortar. The powders were then suspended in ethanol and dispersed onto a carbon-coated copper grid. Selected area electron diffraction (SAED) and high-resolution TEM (HRTEM) were carried out using (Tecnai G2 F20, FEI Co., Hillsboro, OR).

The relative dielectric constant ε_r and the temperature coefficient of resonance frequency τ_f were measured by the Hakki-Coleman method[25] with a network analyzer (E8363B, Agilent Technologies Inc., Palo Alto, CA). The measurement of τ_f was organized in the temperature range of 20 – 80^{o}C. The quality factor Q was evaluated by the resonant-cavity method,[26] using a silver-coated cavity connected to the network analyzer. As the Q-factor generally varied inversely with frequency (f) in the microwave range, the product $Q\times f$, rather than Q alone, was used to evaluate the dielectric loss.

The infrared reflectivity spectra were measured using a Fourier transform infrared spectrometer (IFS 66v/S Vacuum, Bruker Optik GmbH, Ettlingen, Germany) covering far-infrared (80-700 cm^{-1}) and middle-infrared (550-6000 cm^{-1}), respectively. In the far-infrared region, the spectrometer was configured with a Mylar-multilayer beam splitter and PE-DTGS (Bruker, Ettlingen, Germany) detector while a Ge/KBr beam splitter (Bruker) and DTGS detector were utilized in the middle-infrared region. The far and middle infrared spectra agreed well with each other in the

overlapped frequency region. The spectral resolution was selected as 2 cm^{-1} and the incident angle of light was fixed at 12°. A highly reflective mirror was used as reference.

3 Results and discussions

In the present work, much care has to be taken with the synthesis of $Sr_2LaAlTiO_7$ Ruddlesden-Popper phases as they are often close in energy to the other members of the series, as well as the perovskite phase.[27] Fig. 1 shows the XRD patterns of $Sr_2LaAlTiO_7$ powders synthesized by directly heating stoichiometric amounts of $SrCO_3$, La_2O_3, Al_2O_3 and TiO_2 up to 1600°C for 6h. Some minor diffraction peaks corresponding to the $Sr_2LaAlTiO_7$ are observed, while accompanied by strong peaks of $Sr_{1.5}La_{0.5}Al_{0.5}Ti_{0.5}O_4$ and $Sr_{0.5}La_{0.5}Al_{0.5}Ti_{0.5}O_3$ impurities. Similar results are also reported in other groups and the common methods to eliminate the impurities are by extending the sintering time to several days.[20–23,27,28] However, owing to the factor of cost, long time sintering is difficult to implement real applications, and an alternative synthesis pathway should be developed.

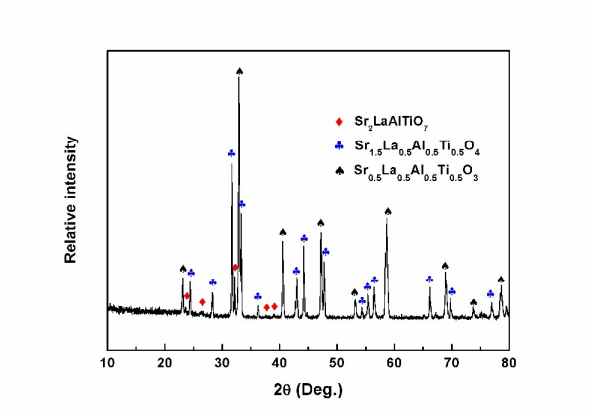

Fig. 1 XRD patterns of $Sr_2LaAlTiO_7$ powders synthesized by directly heating stoichiometric raw powders to 1600°C for 6h.

Considering that the end members ($SrLa_2Al_2O_7$ and $Sr_3Ti_2O_7$) have been successfully prepared with relative simpler sintering condition. These two intermediate compounds are firstly prepared and then mixed according to the nominal composition $Sr_2LaAlTiO_7$. Fig. 2 shows the corresponding XRD patterns synthesized at their optimal temperature. All the patterns indicate the major phase with n = 2 RP structure, implying that $Sr_2LaAlTiO_7$ have been successfully prepared by forming a solid solution between $SrLa_2Al_2O_7$ and $Sr_3Ti_2O_7$. Although some diffraction peaks corresponding to the previous obtained impurities are still observed in Fig. 2(c), their intensities are much lower when compared to those in Fig. 1.

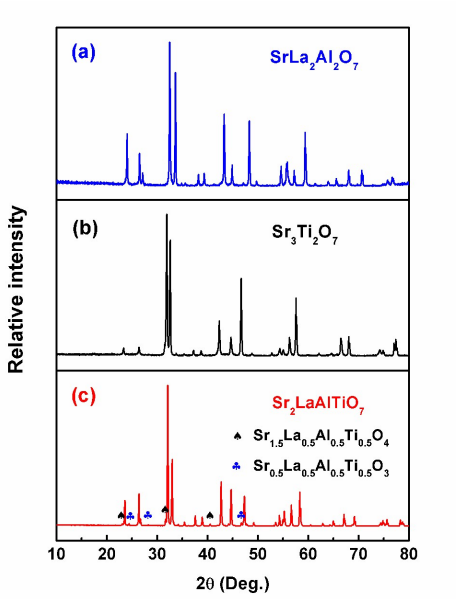

Fig. 2 XRD patterns of $SrLa_2Al_2O_7$ (a) and $Sr_3Ti_2O_7$ (b) end members and $Sr_2LaAlTiO_7$ ceramics (c) synthesized at their optimal temperatures.

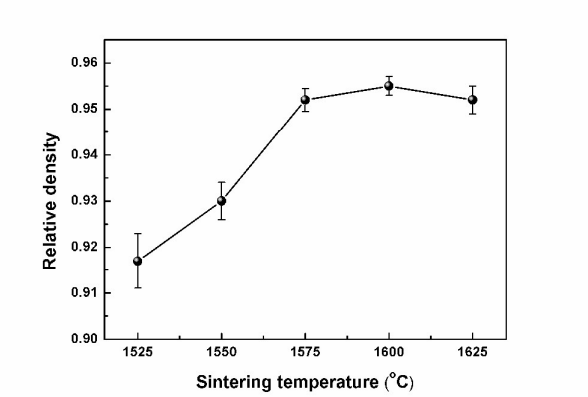

Fig. 3 Relative density of $Sr_2LaAlTiO_7$ ceramics as a function of sintering temperature.

Fig. 3 shows the relative density of $Sr_2LaAlTiO_7$ ceramics as a function of sintering temperature. The density ascends gradually with increasing sintering temperature, reaches the maximum at 1600°C, and then decreases slightly when sintered 1625°C. SEM images of the polished and thermally etched surfaces are presented in Fig. 4. The grains of all the matrix phase generally exhibit strip-like and/or tabular morphology. An obvious melting of grain boundary due to over-sintering is observed in Fig. 4(e). Besides, as shown in Fig. 4(a), the grain

size scatters around 5 μm and some stacking pores are observed. With increasing sintering temperature, more dense microstructure and larger average grain size are obtained. The increased sintering temperature which results in a larger driving force for grain growth should be the main cause.

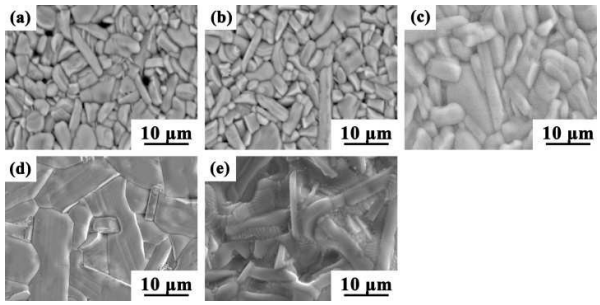

Fig. 4 SEM images of $Sr_2LaAlTiO_7$ ceramics sintered at various temperatures: (a) 1525°C, (b) 1550°C, (c) 1575°C, (d) 1600°C and (e) 1625°C.

To further analysis the structure, the XRD data of $Sr_2LaAlTiO_7$ ceramics are refined on the basis of the $SrLa_2Al_2O_7$ structure with space group *I*4/*mmm* (see Fig. 5(a)). The lattice parameters are calculated as $a = b = 3.840$ Å and $c = 20.270$ Å. Small differences ($R_p = 10.2\%$, $R_{wp} = 13.4\%$, $\chi^2 = 6.77$) between the calculated and experimental intensities for some reflections should be due to the strong preferential orientation of n = 2 RP series.[28] The final structural parameters obtained from the refinement are collected in Table 1 and the resulting structure is depicted in Fig. 5(b). In $Sr_2LaAlTiO_7$ ceramics, there are two sets of A-site (the twelvefold A1 site in the middle of the P slab and the ninefold A2 one in the RS layer), one possible B-site (the center of oxygen octahedral) and three sets of oxygen atoms. Considering that the occupation distribution of A-site cations varies with the composition,[11,27,28] the occupation factors for Sr^{2+}/La^{3+} have been refined and listed in Table 1. It is worth noting that the distributions of A-site cations deviate from the nominal composition, and the larger Sr^{2+} shows a preference for the ninefold A2 site (Sr2). Besides, owing to the layered structure, $Sr_2LaAlTiO_7$ could be viewed as successive layers along *c* axis, i.e. $-(Al_{0.5}Ti_{0.5})O_2-(Sr,La)O-(Sr,La)O-(Al_{0.5}Ti_{0.5})O_2-(Sr,La)^*O-(Al_{0.5}Ti_{0.5})O_2-(Sr,La)O-(Sr,La)O-(Al_{0.5}Ti_{0.5})O_2-$ (see Fig. 5 (b), (Sr,La) with asterisk is twelvefold site and the others are ninefold sites). In this case, the resulting charges per formula unit are not zero and a polarization electric field can be formed between layers. As a result, the internal stress will appear as the apical oxygen anions and A-site cations move oppositely along *c* axis to minimize the interlayer polarization.[29] Using Eq. (1),[11] the formal charges of each layer have been deduced and displayed in Fig. 5(b) accordingly.

$$C = \sum_{i=1} C_i x_i - C_o \quad (1)$$

where, C is the interlayer polarization charge, C_i is the valence of cation, x_i is the proportion of the relevant cation based on the distribution shown in Table 1 and C_O is the formal charge of oxygen. It is worth noting that the interlayer charges of $Sr_2LaAlTiO_7$ ceramics are much smaller when compared to those of $SrLa_2Al_2O_7$ ceramics.[11] The reduced interlayer polarization should indicate a more uniform microstructure and less internal stress in $Sr_2LaAlTiO_7$ ceramics.

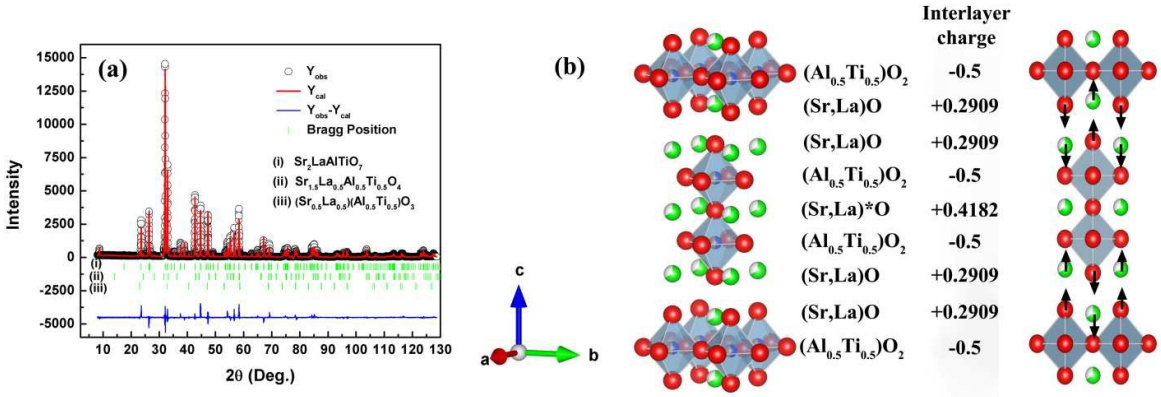

Fig. 5 (a) Profiles fits for the Rietveld refinement of $Sr_2LaAlTiO_7$ dense ceramics. (b) Crystal structure of $Sr_2LaAlTiO_7$ ceramics and the atomic distributions along *c* axis representing interlayer polarization. The values of interlayer charges are also listed.

Table 1 Refined atomic coordinates, thermal displacement parameters and occupations for $Sr_2LaAlTiO_7$ ceramics

Atomic	Site	*x*	*y*	*z*	Biso.	Occupations
Sr1	2*b*	0.00000	0.00000	0.50000	1.253(36)	0.5806
La1	2*b*	0.00000	0.00000	0.50000	1.303(38)	0.4194
Sr2	4*e*	0.00000	0.00000	0.31631(4)	1.288(25)	1.4194
La2	4*e*	0.00000	0.00000	0.31631(4)	1.288(25)	0.5806
Al	4*e*	0.00000	0.00000	0.09622(12)	1.176(51)	1
Ti	4*e*	0.00000	0.00000	0.09622(12)	1.176(51)	1
O1	2*a*	0.00000	0.00000	0.00000	1.017(68)	1
O2	8*g*	0.00000	0.50000	0.09520(20)	1.017(68)	4
O3	4*e*	0.00000	0.00000	0.19649(29)	1.017(68)	2

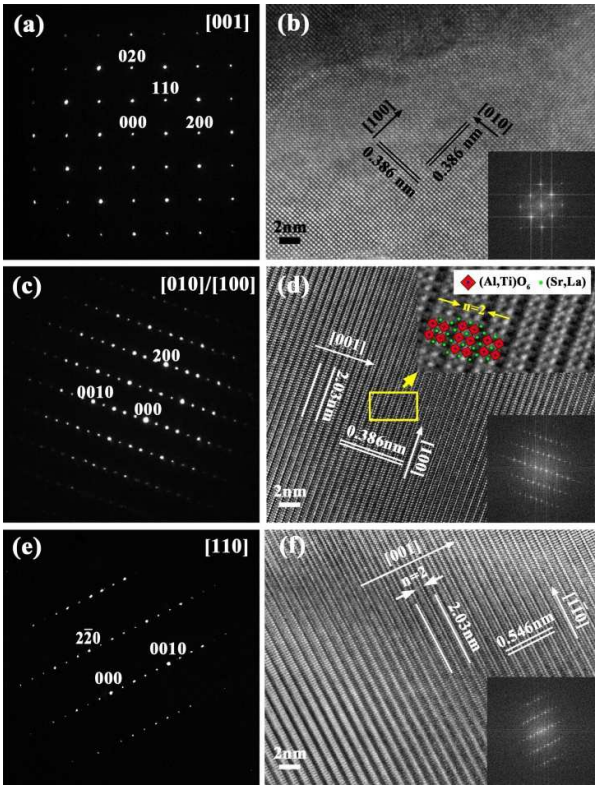

Fig. 6 SAED patterns and corresponding HRTEM images in [001], [010], [110] zone axis for $Sr_2LaAlTiO_7$ ceramics. The simulated diffraction pattern of HRTEM images using FFT are also shown in the inset.

In order to get more complete structural information, Fig. 6 gives the SAED patterns parallel to [001], [010], [110] zone axes and the corresponding HRTEM images of $Sr_2LaAlTiO_7$ ceramics sintered at 1600°C. All these three SAED patterns demonstrate clean and sharp diffraction spots and no mottled contrast is observed. Besides, these patterns could be ideally indexed according to the tetragonal model in space group *I*4/*mmm*. As the [010] patterns are essentially identical to the [100] patterns, the SAED patterns in Fig. 6(c) have been labeled as both but, to avoid confusion, indexed only as [010]. Besides, good agreements between the interplanar distance and the refined lattice constants are obtained in the HRTEM images, which further confirm the crystal structure. Moreover, for n ≥ 2 RP series, defects involving stacking faults between perovskite and rock-salt blocks are always present, which is notoriously detrimental to their properties.[29–31] In the present work, much care has been taken to the lattice images along the [010] zone axis, as it is the most readily interpretable direction for direct observation of lattice disorder. The HRTEM image in Fig. 6(d) displays an uninterrupted periodicities of 2.03 and 0.386 nm, suggesting an ordered n = 2 term. To distinctly exhibit the stacking layer structure, larger magnification image of the area in the rectangular is shown in the inset, where a well ordered distribution of two perovskite and one rock-salt block, according to an ideal n=2 unit cell is observed. Similarly, long range structural ordering is also obtained in Fig. 6(f), which further confirms the well-ordered stacking structure in $Sr_2LaAlTiO_7$ ceramics.

Fig. 7 gives the microwave dielectric properties of $Sr_2LaAlTiO_7$ ceramics sintered at various temperatures. The variation of ε_r presents a similar variation trend with the relative density, implying that the dielectric constant of the present ceramics is predominantly dominated by the relative density. The maximum dielectric constant of the $Sr_2LaAlTiO_7$ ceramics is adjusted to 26.5, which is higher than that of $Ba(Mg_{1/3}Ta_{2/3})O_3$.

The temperature coefficient of resonant frequency (τ_f) is related to the temperature coefficient of ε_r (τ_ε) and the linear thermal expansion coefficient α_L by the following equation:[32,33]

$$\tau_f = -(\tau_\varepsilon/2 + \alpha_L) \quad (2)$$

where, the value of α_L is almost a constant about 10 ppm/°C.[34] Therefore, for the present system without tilting of the octahedral, τ_f is mainly tuned by τ_ε which is closely related to ε_r. Consequently, the τ_f of the present ceramics shifts gradually towards the positive direction with increasing sintering temperature, and shows a nearly same trend as ε_r. Besides, it is worth noting that all the compositions exhibit an acceptable τ_f value no larger than ±3 ppm/°C, which satisfies the requirement for microwave devices.[35]

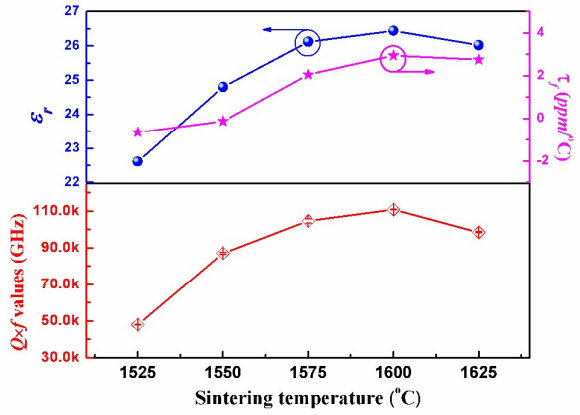

Fig. 7 The microwave dielectric properties of $Sr_2LaAlTiO_7$ ceramics as a function of sintering temperature.

$Q\times f$ value increases with the sintering temperature until it reaches the maximum (110,850 GHz) at 1600°C and decreases thereafter due to over-sintering. The improvement of $Q\times f$ value for samples sintered at 1600°C can be associated with the increase of relative density as the existence of pores is notoriously detrimental. On the other hand, the increased grain size is also beneficial as it is commonly deemed that larger grain size results in less grain boundary which indicates fewer lattices mismatch and lower dielectric loss.[36] What is more, the reduced interlayer polarization and the well-ordered stacking structure as we discussed above should also play a beneficial part in obtaining the high $Q\times f$ value. Even though the $Q\times f$ value of $Sr_2LaAlTiO_7$ ceramics is smaller than that of $Ba(Mg_{1/3}Ta_{2/3})O_3$, the merits of easier preparation, less process sensitivity and most importantly, the comparatively cheap raw materials should outweigh the disadvantage. The optimal combination of microwave dielectric properties is obtained as: ε_r = 26.5, $Q\times f$ = 110,850 GHz, τ_f = 2.95 ppm/°C, and this indicates that $Sr_2LaAlTiO_7$ ceramics can be expected as promising new candidate for ultra-low loss microwave dielectric ceramics.

Furthermore, the IR reflectivity spectra of $Sr_2LaAlTiO_7$ ceramics are analyzed to understand their intrinsic dielectric properties. The obtained IR reflectivity spectra are related to complex dielectric function $\varepsilon^*(\omega)$ by the following relation:[37]

$$R(\omega) = \left| \frac{\sqrt{\varepsilon^*(\omega)} - 1}{\sqrt{\varepsilon^*(\omega)} + 1} \right|^2 \quad (3)$$

According to the classical oscillator model,[38] the complex dielectric function $\varepsilon^*(\omega)$ can be written as:

$$\varepsilon^*(\omega) = \varepsilon_\infty + \sum_{j=1}^{n} \frac{S_j(\omega_j^2 - \omega^2)}{(\omega_j^2 - \omega^2)^2 + \omega^2\gamma_j^2} - i\sum_{j=1}^{n} \frac{S_j\omega\gamma_j}{(\omega_j^2 - \omega^2)^2 + \omega^2\gamma_j^2}$$
$$= \varepsilon'(\omega) - i\varepsilon''(\omega) \quad (4)$$

where, n is the number of transverse polar-phonon modes; ω_j , S_j, and γ_j are the eigen frequency, strength, and damping constant of the j-th mode, respectively; ε_∞ is the dielectric constant caused by the electronic polarization at the optical frequency. By using K-K relations, the IR reflectivity spectra were transformed into the complex dielectric spectra,[37] and the obtained image part spectra were fitted with $\varepsilon''(\omega)$ in Eq. 4 to determine the initial values of ω_j , S_j, and γ_j. The initial value of ε_∞ was calculated from the reflectivity at 6000 cm^{-1} using Eq. 3. With these initial values acquired, the microwave dielectric constant and loss tangent can be estimated under the condition of $\omega << \omega_j$:

$$\varepsilon'(\omega) \approx \varepsilon_\infty + \sum_{j=1}^{n} \frac{S_j}{\omega_j^2} = \varepsilon_\infty + \sum_{j=1}^{n} \Delta\varepsilon'_j \quad (5)$$

$$\varepsilon''(\omega) \approx \sum_{j=1}^{n} \frac{\omega\gamma_j S_j}{\omega_j^4} \quad (6)$$

$$\tan\delta = \frac{\varepsilon''(\omega)}{\varepsilon'(\omega)} = \sum_{j=1}^{n} \Delta\tan\delta_j \approx \sum_{j=1}^{n} \frac{\omega}{\varepsilon'(\omega)} \frac{S_j\gamma_j}{\omega_j^4} \quad (7)$$

where, $\Delta\varepsilon'_j$ and $\Delta\tan\delta_j$ denote the contributions of the j-th mode to the dielectric constant and dielectric loss, respectively.

The IR reflectivity spectra of $Sr_2LaAlTiO_7$ ceramics have been measured and fitted using classical oscillator model (see Fig. 8 (a)) and the calculated complex dielectric responses (ε' and ε") are shown in Fig. 8 (b) and (c), respectively. The measured dielectric constant and dielectric loss are also plotted (solid circles) to compare with the calculated ones. It is worth note that the calculated dielectric constant is a little smaller than the measured value, which is similar with the results reported in $SrLn_2Al_2O_7$ (Ln = Nd, Sm) ceramics.[19]

The reason should associate with the extrinsic contributions from the defect phonon scattering in the measured microwave frequency.[39] The calculated and measured dielectric losses have the same order of magnitudes, implying that the majority dielectric loss at microwave region is attributed to the absorptions of structural phonon oscillation at infrared region.[40,41] The phonon parameters obtained from the fitting of the infrared reflectivity spectra are listed in Table 2. The vibration modes below 350cm^{-1} (especially the two modes of j = 1 and 3) give the primary contribution to the microwave dielectric constant (54%) and dielectric loss (81%). The dominant contribution of lower frequency modes to complex dielectric responses is based on the fact that for a given effective charge of a polar phonon mode, its contributions are $\Delta\varepsilon'_j \propto S_j\omega_j^{-2}$, and $\Delta\tan\delta_j \propto S_j\gamma_j\omega_j^{-4}$,[13,19] and they decrease very fast with increasing ω_j. The theoretical $Q\times f$ values calculated from the sum of dielectric loss is 120,554 GHz, indicating that there is still some space for the increase of $Q\times f$ value in the present ceramics. As some minor impurities still exist, which are notoriously poisonous, further improvement of the properties should be expected through compositional modification, especially by suppressing the impurities.

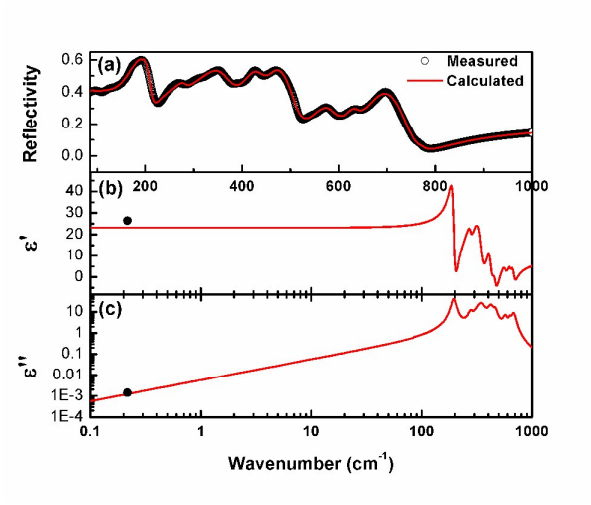

Fig. 8 (a) Measured and calculated infrared reflectivity spectra of $Sr_2LaAlTiO_7$ ceramics; (b, c) the real and imaginary part of complex responses obtained from the fitting of IR reflectivity spectra (the solid circles are the experimental value at microwave region).

4 Conclusions

$Sr_2LaAlTiO_7$ ceramics have been successfully prepared via a relatively simple process. XRD and SAED results reveal the formation of n = 2 Ruddlesden–Popper structure with space group *I*4/*mmm*. The SEM micrographs indicate a more dense microstructure and larger grain size when sintered at 1600°C, where well ordered intergrowths between perovskite and rock-salt blocks are also confirmed by HRTEM observation. Excellent microwave dielectric properties (especially ultra-high $Q\times f$ value) can be obtained in the present ceramics, and the best combination of microwave dielectric characteristics is obtained as: ε_r = 26.5, $Q\times f$ = 110,850 GHz, τ_f = 2.95 ppm/°C, which are much better than those for $MLnAlO_4$ and $SrLn_2Al_2O_7$, and almost compete with those for $Ba(Mg_{1/3}Ta_{2/3})O_3$. Considering the merits of easier preparation, less process sensitivity and most importantly, the comparatively cheap raw materials, $Sr_2LaAlTiO_7$ ceramics can be expected as a promising new candidate for ultra-low loss microwave dielectric ceramics.

Table 2 Phonon parameters obtained from the fitting of the infrared reflectivity spectra of $Sr_2LaAlTiO_7$ ceramics

j	ω_j	γ_j	$\Delta\varepsilon'_j$	$\Delta\tan\delta_j\times10^4$ at 10GHz
1	196.21	17.60	5.27	0.2720
2	280.25	30.27	0.89	0.0364
3	346.66	62.79	6.59	0.3631
4	421.25	49.22	2.19	0.0847
5	463.21	49.32	1.60	0.0409
6	570.11	56.94	0.73	0.0138
7	632.56	52.97	0.49	0.0062
8	682.77	57.73	0.64	0.0124
ε_∞			5.38	0.0000
$\sum$			23.78	0.8295

Acknowledgements

The present work was financially supported by Chinese National Basic Research Program under grant number 2015CB654601.

References

1 T. A. Vanderah, *Science*, 2002, **298**, 1182.

2 I. M. Reaney and D. Iddles, *J. Am. Ceram. Soc.*, 2006, **89**, 2063.

3 C. F. Tseng, *J. Am. Ceram. Soc.*, 2008, **91**, 4125.

4 J. Xue, S. Wu and J. Li, *J. Am. Ceram. Soc.*, 2013, **96**, 2481.

5 C. W. Zheng, S. Y. Wu, X. M. Chen, and K. X. Song, *J. Am. Ceram. Soc.*, 2007, **90**, 1483.

6 S. Nomura, K. Toyama, and K. Kaneta, *Jpn. J. Appl. Phys.*, 1982, **21**, 624.

7 H. Hughes, D. M. Iddles and I. M. Reaney, *Appl. Phys. Lett.*, 2001, **79**, 2952.

8 L. Yi, L. Li, X. Q. Liu, and X. M. Chen, *J. Am. Ceram. Soc.*, 2014, **97**, 3531.

9 S. George and M. T. Sebastian, *J. Am. Ceram. Soc.*, 2010, **93**, 2164.

10 C. Huang and M. Weng, *Mater. Res. Bull.*, 2001, **36**, 2741.

11 L. Yi, X. Q. Liu, L. Li, and X. M. Chen, *Int. J. Appl. Ceram. Tec.*, 2013, **10**, 177.

12 X. M. Chen, Y. Xiao, X. Q. Liu, and X. Hu, *J. Electroceram.*, 2003, **10**, 111.

13 X. C. Fan, X. M. Chen, and X. Q. Liu, *Chem. Mater.*, 2008, **20**, 4092.

14 L. Guan, M. Li, X. Li, L. Feng, F. Teng, B. Liu, Z. Wei, and C. B. Musgrave, *Comp. Mater. Sci.*, 2015, **96**, 223.

15 Y. Xiao, X. M. Chen and X. Q. Liu, *J. Am. Ceram. Soc.*, 2004, **87**, 2143.

16 H. X. Yuan, X. M. Chen and M. M. Mao, *J. Am. Ceram. Soc.*, 2009, **92**, 2286.

17 M. M. Mao, X. M. Chen, and X. Q. Liu, *J. Am. Ceram. Soc.*, 2011, **94**, 3948.

18 C. Zhang, L. Yi, L. Li, and X. M. Chen, *Int. J. Appl. Ceram. Tec.*, 2013, **10**, 70.

19 L. Yi, X. Q. Liu, and X. M. Chen, *Int. J. Appl. Ceram. Tec.*, 2014, DOI:10.1111/ijac.12366.

20 D. Singh and R. Singh, *J. Electron. Mater.*, 2012, **41,** 540.

21 D. Singh and R. Singh, *J. Chem. Sci.*, 2010, **122**, 807.

22 T. I. Chupakhina and G. V. Bazuev, *Russ. J. Inorg. Chem.*, 2008, **53**, 681.

23 I. B. Sharma, S. K. Magotra, D. Singh, S. Batra, and K. Mudher, *J. Alloy Compd.*, 1999, **291**, 16.

24 J. Rodríguez-Carvajal, *Int. Union Crystallogr. Newsletter.*, 2001, **26**, 12.

25 B. W. Hakki and P. D. Coleman, *IEEE Trans. Microw. Theory Tech.*, 1960, **8,** 402.

26 X. C. Fan, X. M. Chen, and X. Q. Liu, *IEEE Trans. Microw. Theory Tech.*, 2005, **53**, 3130.

27 M. A. Green and D. A. Neumann, *Chem. Mater.*, 2000, **12,** 90.

28 L. Ruiz-Gonzalez, D. Gonzalez-Merchante, R. Cortes-Gil, J. M. Alonso, J. L. Martinez, A. Hernando, and J. M. Gonzalez-Calbet, *Chem. Mater.*, 2015, **27**, 1397.

29 L. Yi, X. Q. Liu, L. Li, and X. M. Chen, *Mater. Chem. Phys.*, 2014, **147**, 162.

30 J. Sloan, P. D. Battle, M. A. Green, M. J. Rosseinsky, and J. F. Vente, *J. Solid State Chem.*, 1998, **138**, 135.

31 W. Tian, X. Q. Pan, J. H. Haeni, and D. G. Schlom, *J. Mater. Res.*, 2001, **16**, 2013.

32 I. M. Reaney, P. Wise, R. Ubic, J. Breeze, N. M. Alford, D. Iddles, D. Cannell, and T. Price, *Philosophical Magazine A*, 2001, **81**, 501.

33 M. S. Fu, X. Q. Liu, X. M. Chen, and Y. W. Zeng, *J. Am. Ceram. Soc.*, 2008, **91**, 1163.

34 E. L. Colla, I. M. Reaney, and N. Setter, *J. Appl. Phys.*, 1993, **74**, 3414.

35 M. T. Sebastian, in *Dielectric Materials for Wireless Communication*, Elsevier Publishers, Oxford, United Kingdom, 2008.

36 N. Ichinose and T. Shimada, *J. Eur. Ceram. Soc.*, 2006, **26**, 1755.

37 B. Liu, L. Yi, X. Q. Liu, and X. M. Chen, *J. Electroceram.*, 2015, **34**, 114.

38 R. Zurmühlen, J. Petzelt, S. Kamba, V. V. Voitsekhovskii, E. Colla, and N. Setter, *J. Appl. Phys.*, 1995, **77**, 5341.

39 D. Zhou, W. Li, L. Pang, Z. Yue, G. Pang, and X. Yao, *RSC Adv.*, 2015, **5,** 19255.

40 H. H. Xi, D. Zhou, H. D. Xie, B. He, and Q. P. Wang, *J. Am. Ceram. Soc*., 2015, **98**, 587.

41 D. Zhou, W. Li, H. Xi, L. Pang, and G. Pang, *J. Mater. Chem. C*, 2015, **3,** 2582.